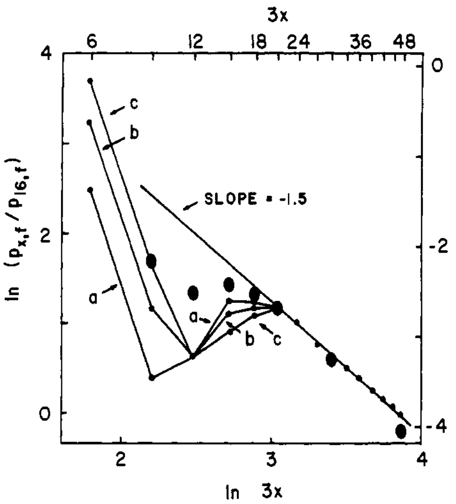

Figure 2. Chain length dependence of normalized cyclization probabilities ($p_{x,f}/p_{16,f}$) and experimental kinetic constants (EM). The values of f used are 0.1, 0.3, and 0.5 for curves a, b, and c, respectively. A straight line of slope −1.5 is drawn through the curves at high x. Kinetic constants are from Illuminati et al.[11] They are depicted as filled ovals.

"end-to-end distance" of 500 pm or less is observed for a chain of specified x when the starting conformation is that depicted in Figure 1B or 1C, respectively. The desired probability, $p_{x,f}$, is then formulated as $p_{x,f} = fp_{x,B} + (1 - f)p_{x,C}$. The most important conclusions reached in this study can be obtained with any physically sensible assignment of f.

Results and Discussion

Figure 2 depicts calculated cyclization propensities using f = 0.1, 0.3, and 0.5. Our concern here is with trends seen upon changes in x. In order to facilitate comparison, the vertical scale in Figure 2 has been adjusted so that points obtained at all f are coincident for the largest molecule studied (x = 16). This objective is obtained by multiplying each $p_{x,f}$ by a constant, $1/p_{16,f}$. The resulting curves are essentially coincident for $x \geq 7$. They are well described by a straight line with slope -1.5, as is shown in Figure 2. This is the slope expected for any sufficiently large flexible chain.[14] The large filled circules in Figure 2 denote the kinetic constants (designated[11] as EM) obtained experimentally by Illuminati et al.[11] for formation of the macrocycles of the type depicted in Figure 1A. Kinetic constants for formation of the larger rings are also described by the straight line of slope -1.5 when x is larger than about 7. Thus the Monte Carlo calculations correctly identify the value of x at which the limiting behavior is obtained. This identification can be obtained with any reasonable assignment for f.

None of the experimental kinetic constants plotted in Figure 2 lie above the extrapolation of the line whose slope is -1.5. Kinetic constants for the shorter chains fall significantly below this line. The three Monte Carlo curves for x between 3 and 6 also fall below the extrapolation of the line whose slope is -1.5. Thus the calculation correctly identifies the direction in which chains of this size deviate from the trends established by the behavior of long chains. Futhermore, the direction in which this deviation occurs is *opposite* to that seen in the absence of the aromatic system. The point for $(OCH_2CH_2)_6$ has been found to lie significantly *above* the trend established by $(OCH_2CH_2)_x$ of large x.[10] Incorporation of the benzo moiety into the crown ether eliminates the enhanced propensity for cyclization to form $(OCH_2CH_2)_6$. This benzo moiety prohibits approximate description of $(OCH_2CH_2)_6$ conformations using a tetrahedral lattice, just as does substitution of sulfur for the oxygen atoms in the macrocycle.[10] Either change therefore abolishes the special ease of formation of the 18-member ring.

The experimental kinetic constants pass through a shallow minimum when x is 4. Monte Carlo calculations also find a minimum near x = 4, although the calculated minimum is somewhat deeper than that found experimentally. The minimum located by the Monte Carlo calculation occurs precisely at x = 4 if f lies between 0.14 and 0.80. A small macrocyclization equilibrium constant was also calculated for $(OCH_2CH_2)_4$[4] and $(SCH_2CH_2)_4$.[10]

In conclusion, the Monte Carlo calculations based on a rotational isomeric state model for unperturbed acyclic poly(oxyethylene) reproduce the following features of the kinetic constants for formation of the ring system depicted in Figure 1A. (1) The limiting behavior is obtained when x is about 7. (2) Cyclization constants at smaller x (x = 2 possibly excepted) fall *below* the prediction based on extrapolation of the limiting behavior. (3) Cyclization constants pass through a minimum when x is near 4. We can therefore infer that the probability for adoption of a conformation with a small "end-to-end distance" makes a dominant contribution to the cyclization rate for these molecules.

Acknowledgment is made to the donors of the Petroleum Research Fund, administered by the American Chemical Society, for the support of this research.

---

[14] Flory, P. J.; Suter, U. W.; Mutter, M. *J. Am. Chem. Soc.* **1976**, *98*, 5733.

Gas-Phase Reactions of Rh$^+$ with Alkanes

G. D. Byrd and B. S. Freiser*

Contribution from the Department of Chemistry, Purdue University, West Lafayette, Indiana 47907. *Received March 8, 1982*

Abstract: The gas-phase reactions of laser-desorbed Rh$^+$ with various alkanes are examined using Fourier transform mass spectrometry (FTMS). The secondary reactions of these product ions are also reported. In contrast to the first-row group 8 transition metal ions whose reactions with alkanes show extensive cleavage of C–C bonds, Rh$^+$ shows few products resulting from C–C cleavage, and dehydrogenation is the major process in all reactions. Evidence is given that suggests the existence of a π-allylic intermediate, and some dehydrocyclization is indicated in our results. Ligands with molecular formulas corresponding to trienes bound to rhodium show no further reaction which may be caused by either steric or electronic effects.

The gas-phase reactions of transition metal ions with various hydrocarbons have been the focus of recent investigations by ion cyclotron resonance (ICR) spectrometry[1-3] and ion beam techniques.[4-7] The results of these experiments have provided many

0002-7863/82/1504-5944$01.25/0

fundamental insights into the mechanisms of organometallic reactions as well as important thermochemical information. Most of the work has involved first-row transition metals with few reports of secondary reaction products because of the limited mass range of conventional ICR and the inability of ion beam instruments to trap ions long enough to observe secondary reaction products.

The recent application of Fourier transform techniques to ICR mass spectrometry (FTMS) has expanded the capabilities of this method[8] with regard to both mass range and resolution. These features allow monitoring of secondary reactions which can provide information as to the structure of the primary ions formed as well as increasing our knowledge of the chemistry of these metal complexes.[9] As an additional advantage, when used in conjunction with laser desorption, FTMS can produce a complete spectrum with good signal-to-noise from one laser shot. This improves the reproducibility of the product ion distribution by partially compensating for varying metal ion intensities from one laser shot to the next during signal averaging.

Rhodium, one of the platinum metals, is used in a variety of catalytic reactions involving hydrocarbons.[10] Various metallic catalysts, including rhodium complexes, have been developed primarily by the petroleum industry for use in hydrogenation and dehydrogenation reactions,[11] an area of increasing expansion as new and more efficient catalytic materials are sought. While much investigation has been focused on the condensed phase and at catalytic surfaces, little has been done on the fundamental reactions in the gas phase between rhodium and organic species. We report here the reactions of laser-desorbed Rh^+ with various alkanes in the gas phase as determined by FTMS. Multiple dehydrogenation dominates both primary and subsequent reactions, and evidence is given that suggests the formation of π-allyl species bound to the metal.

Experimental Section

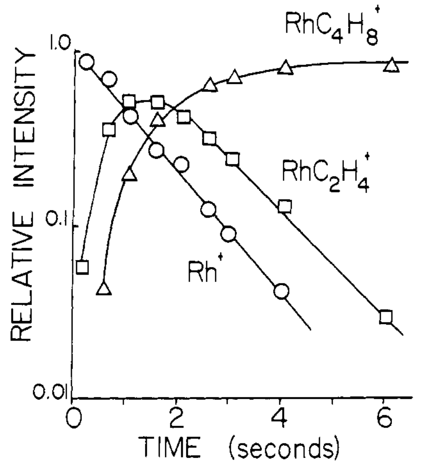

Figure 1. Temporal variation of ion abundance for the Rh^+–ethane system. The pressure is 1×10^{-7} torr.

Scheme I

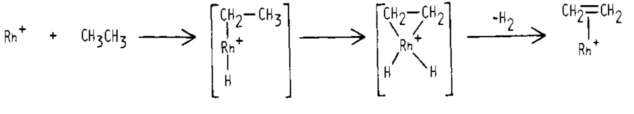

The reactions described in this paper were carried out using a prototype Nicolet FTMS-1000 previously described in detail[12] which has a 1-in. cubic trapped ion cell situated between the poles of a Varian 15-in. electromagnet maintained at 0.9 T. The cell has been modified by drilling a 0.25-in. hole in one of the receiver plates to give various light sources access to the inside of the cell. The frequency doubled beam (530 nm) of a Quanta Ray Nd:YAG laser was focused on the opposite plate which supported a 1-mm thick foil of pure rhodium.

The distributions of primary product ions listed in Table I were measured from the mass spectra when secondary products were barely observable (<5% of the most intense peak). The listed values for the primary products are reproducible to within ±10% absolute. Secondary reaction pathways for the major primary product ions (>10% of the total products) were determined by double resonance techniques[13] and are also listed in Table I. Like many ionization techniques, laser desorption is susceptible to the formation of ions in excited states.[14] We have previously shown that the majority of the metal ions monitored by our experiment are in their ground state.[30] Some of the smaller reactions listed in Table I, however, may result from reactions of excited-state rhodium cation, but no evidence of such reactions is given here. Sample pressures were on the order of 1×10^{-7} torr and were monitored with a Bayard-Alpert ionization gauge. The measured rate constants for the primary reactions varied from 40 to 80% of the Langevin value. Deuterium exchange reactions were carried out by increasing the total pressure in the system to $\sim 10^{-6}$ torr with D_2. All chemicals used were high-purity commercial samples used as supplied except for multiple freeze–pump–thaw cycles.

Results and Discussion

Table I lists the product distributions for all of the primary Rh^+/alkane interactions as well as the major subsequent reactions of the product ions. The primary products agree qualitatively with those reported in a preliminary study of Rh^+ produced by electron impact on $CpRh(CO)_2$.[15] In general, loss of one or more hydrogen molecules (H_2) from the ion–molecule collision complex dominates both primary and secondary reactions for all alkanes. While small amounts of C–C cleavage products are seen for normal alkanes larger than butane, certain branched alkanes react with Rh^+ to release considerable amounts of smaller alkanes. The ring skeletons of the cycloalkanes tend to remain intact and multiple H_2 losses dominate.

The initial step in dehydrogenation reactions is believed to be insertion by the metal into a C–H bond followed by a β-hydride shift and reductive elimination of H_2. This is illustrated in Scheme I where a metal–ethylene complex is produced from the reaction of Rh^+ with ethane. As shown below, larger alkanes often permit a second C–H insertion and β-hydride shift accounting for subsequent H_2 losses. This mechanism explains most of the major reactions in Table I but must be modified when β-hydride shifts are blocked by branching on the carbon chain. The alkanes are grouped below on the basis of similar behavior and discussed.

Ethane. C_2H_6 is the smallest alkane observed to react with Rh^+ (neither CH_4 nor H_2 gave any products), and the secondary reaction of $RhC_2H_4^+$ mimics the primary reaction. Loss of H_2 can be explained by Scheme I for both reactions. The ethylene

---

(1) (a) R. C. Burnier, G. D. Byrd, and B. S. Freiser, *J. Am. Chem. Soc.*, **103**, 4360 (1980); (b) *Anal. Chem.*, **52**, 1641 (1980).

(2) (a) J. Allison and D. P. Ridge, *J. Am. Chem. Soc.*, **101**, 4998 (1979); (b) J. Allison, R. B. Freas, and D. P. Ridge, *ibid.*, **101**, 1332 (1979).

(3) R. W. Jones and R. H. Staley, *J. Am. Chem. Soc.*, **102**, 3794 (1980).

(4) (a) P. B. Armentrout and J. L. Beauchamp, *Chem. Phys.*, **48**, 315 (1980); (b) *ibid.*, **50**, 37 (1980).

(5) P. B. Armentrout and J. L. Beauchamp, *J. Am. Chem. Soc.*, **103**, 784 (1981).

(6) P. B. Armentrout, L. F. Halle, and J. L. Beauchamp, *J. Am. Chem. Soc.*, **103**, 6501 (1981).

(7) (a) P. B. Armentrout, L. F. Halle, and J. L. Beauchamp, *J. Am. Chem. Soc.*, **103**, 6624 (1981); (b) P. B. Armentrout and J. L. Beauchamp, *ibid.*, **103**, 6628 (1981).

(8) (a) A. B. Marshall, M. B. Comisarow, and G. Parisod, *J. Chem. Phys.*, **71**, 4434 (1979); (b) M. B. Comisarow, *Int. J. Mass Spectrom. Ion Phys.*, **37**, 251 (1981).

(9) G. Parisod and M. B. Comisarow, *Adv. Mass Spectrom.*, **8**, 212 (1980).

(10) F. A. Cotton and G. Wilkinson, "Advanced Inorganic Chemistry", 4th ed., Wiley-Interscience, New York, 1980, pp. 901–904.

(11) D. A. Dowden in "Catalysis", (Specialists Periodical Report), Vol. 2, C. Kemball and D. A. Dowden, Eds., The Chemical Society, London, 1977, pp 1–27.

(12) R. B. Cody, R. C. Burnier, and B. S. Freiser, *Anal. Chem.*, **54**, 96 (1982).

(13) M. B. Comisarow, V. Grassi, and G. Parisod, *Chem. Phys. Lett.*, **57**, 413 (1978).

(14) J. F. Ready, "Effects of High-Powered Laser Radiation", Academic Press, New York, 1971.

(15) M. Mandich and J. L. Beauchamp, 1982 Western Regional Conference on Gaseous Ion Chemistry, Lake Arrowhead, Calif.

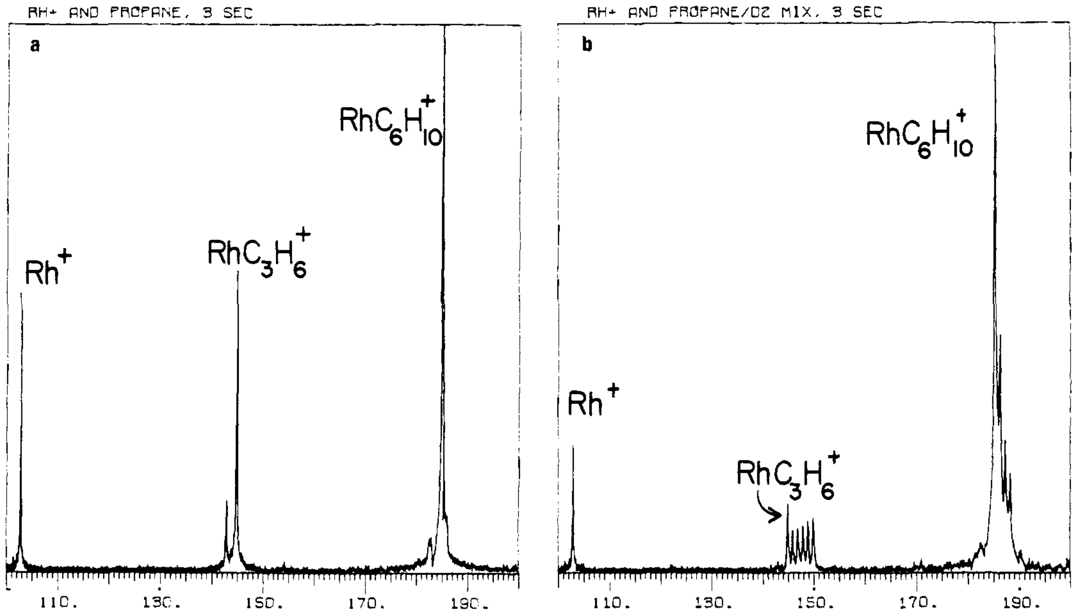

Figure 2. Fourier-transformed mass spectra of the Rh^+–propane system after 3 s: (a) without D_2 and (b) with 10^{-6} torr of D_2. The pressure of the propane in both cases is 1×10^{-7} torr and each spectrum is the result of one transient from a single laser shot.

Scheme II

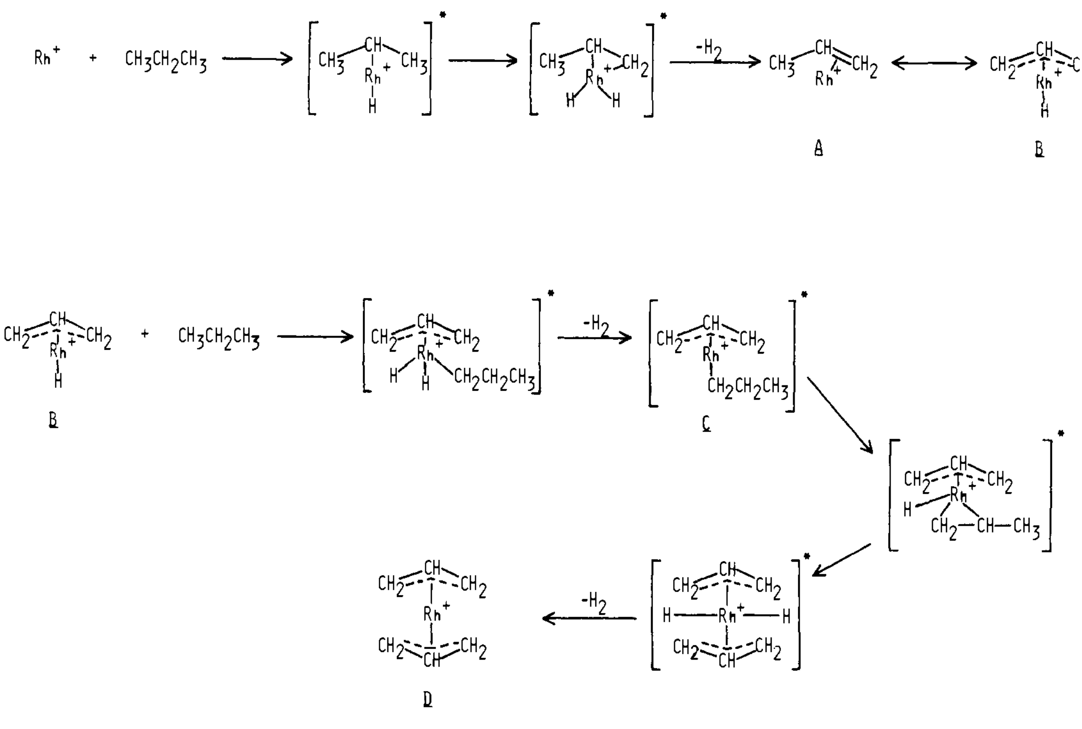

ligand attached to Rh^+ apparently does little to hamper a second oxidative addition by the metal as shown in Figure 1 where both Rh^+ and $RhC_2H_4^+$ react with C_2H_6 at similar rates. The $RhC_4H_8^+$ produced in the latter reaction was not observed to further react with C_2H_6. This is probably due to the steric blocking by two ethylene ligands rather than any electronic saturation since more highly saturated ligands readily undergo secondary reactions as shown below. The exothermic formation of $RhC_2H_4^+$ in this reaction implies that $D(Rh^+–C_2H_4) > 33$ kcal/mol.[16] This result can be compared to $D(Co^+–C_2H_4) = 37 \pm 2$ kcal/mol reported by Armentrout and Beauchamp.[7b]

Propane and 2-Methylpropane. These alkanes have a C_3 chain as a common feature which tends to remain intact in all primary and secondary reactions. Although propane loses one H_2 in its primary reaction with Rh^+ as ethane did, it shows a double H_2 loss in the secondary reaction. This suggests that $RhC_3H_6^+$ is not a simple metal–propene structure and may involve rearrangement to a metal hydride complex. Scheme II incorporates this idea in a mechanism involving a π-allyl hydride species. π-Allyl intermediates play an important role in several mechanisms for alkene isomerization and hydrogenation on metal surfaces[17] and are implicated in our gas-phase work. The $RhC_3H_6^+$ complex results from the primary reaction similar to the ethane case in Scheme I but now A in Scheme II rearranges to the allyl–metal hydride structure B. The metal in this complex again readily inserts into the C–H bond of a second C_3H_8 which provides for immediate hydrogen coupling with the hydride on the metal and

---

(16) This calculation is based on heats of formation taken from H. M. Rosenstock, D. Draxl, B. W. Steiner, and J. T. Herron, *J. Phys. Chem. Ref. Data*, **6**, Suppl. 1 (1977).

(17) G. Webb in ref 11, pp 151–163.

Table I. Listing of Neutrals and Ions Resulting from the Primary and Secondary Reactions of Rh^+ with Various Alkanes[a]

alkane	primary reaction $Rh^+ + \text{alkane} \rightarrow RhA^+ + \text{neutral(s)}$			secondary reaction $RhA^+ + \text{alkane} \rightarrow RhB^+ + \text{neutral(s)}$	
	neutral(s)	RhA^+	rel %	neutral(s)	RhB^+
CH_4		no reaction			
C_2H_6	H_2	$RhC_2H_4^+$	100	H_2	$RhC_4H_8^+$
C_3H_8	H_2	$RhC_3H_6^+$	94	$2H_2$	$RhC_6H_{10}^+$
	$2H_2$	$RhC_3H_4^+$	6	$2H_2$	$RhC_6H_8^+$
n-C_4H_{10}	$2H_2$	$RhC_4H_6^+$	100	$2H_2$	$RhC_8H_{12}^+$
i-C_4H_{10}	H_2	$RhC_4H_8^+$	43	$2H_2$	$RhC_8H_{14}^+$
	$2H_2$	$RhC_4H_6^+$	48	$2H_2$	$RhC_8H_{12}^+$
	CH_4	$RhC_3H_4^+$	9		
n-C_5H_{12}	$2H_2$	$RhC_5H_8^+$	88	$2H_2$	$RhC_{10}H_{16}^+$
	$3H_2$	$RhC_5H_6^+$	4		
	C_2H_6	$RhC_3H_6^+$	4		
	H_2, C_2H_6	$RhC_3H_4^+$	4		
i-C_5H_{12}	$2H_2$	$RhC_5H_8^+$	97	$2H_2$	$RhC_{10}H_{16}^+$
	C_2H_6	$RhC_3H_6^+$	3		
neo-C_5H_{12}	H_2	$RhC_5H_{10}^+$	15	H_2, CH_4	$RhC_9H_{16}^+$
	$2H_2$	$RhC_5H_8^+$	29	$2H_2$	$RhC_{10}H_{16}^+$
				H_2, CH_4	$RhC_9H_{14}^+$
	$3H_2$	$RhC_5H_6^+$	2		
	CH_4	$RhC_4H_8^+$	13	H_2, CH_4	$RhC_8H_{14}^+$
	H_2, CH_4	$RhC_4H_6^+$	34	-	$RhC_9H_{18}^+$
				H_2, CH_4	$RhC_8H_{12}^+$
	C_2H_6	$RhC_3H_6^+$	5	H_2, CH_4	$RhC_7H_{12}^+$
	H_2, C_2H_6	$RhC_3H_4^+$	2		
n-C_6H_{14}	$2H_2$	$RhC_6H_{10}^+$	49	H_2	$RhC_{12}H_{22}^+$
				$2H_2$	$RhC_{12}H_{20}^+$
	$3H_2$	$RhC_6H_8^+$	33	$2H_2$	$RhC_{12}H_{18}^+$
	$4H_2$	$RhC_6H_6^+$	18	$2H_2$	$RhC_{12}H_{16}^+$
$(CH_3)_2CHCH(CH_3)_2$	$2H_2$	$RhC_6H_{10}^+$	100	$2H_2$	$RhC_{12}H_{20}^+$
$(CH_3)_3CCH_2CH_3$	H_2	$RhC_6H_{12}^+$	3		
	$2H_2$	$RhC_6H_{10}^+$	16	-	$RhC_{12}H_{24}^+$
				H_2	$RhC_{12}H_{22}^+$
	$3H_2$	$RhC_6H_8^+$	3		
	H_2, CH_4	$RhC_5H_8^+$	57	H_2	$RhC_{11}H_{20}^+$
				$2H_2$	$RhC_{11}H_{18}^+$
	$2H_2, CH_4$	$RhC_5H_6^+$	8		
	C_2H_6	$RhC_4H_8^+$	7		
	H_2, C_2H_6	$RhC_4H_6^+$	6		
n-C_7H_{16}	$3H_2$	$RhC_7H_{10}^+$	94		
	H_2, C_2H_6	$RhC_5H_8^+$	1		
	H_2, C_3H_8	$RhC_4H_6^+$	5	$2H_2$	$RhC_{11}H_{18}^+$
n-C_8H_{18}	$3H_2$	$RhC_8H_{12}^+$	91		
	$4H_2$	$RhC_8H_{10}^+$	5		
	H_2, C_2H_6	$RhC_6H_{10}^+$	2		
	H_2, C_3H_8	$RhC_5H_8^+$	2		
c-C_3H_6	-	$RhC_3H_6^+$	6	$2H_2$	$RhC_6H_8^+$
	H_2	$RhC_3H_4^+$	76	$2H_2$	$RhC_6H_6^+$ [b]
	CH_2	$RhC_2H_4^+$	3		
	CH_4	$RhC_2H_2^+$	4		
	C_2H_4	$RhCH_2^+$	11	$2H_2$	$RhC_4H_4^+$
c-C_4H_8	H_2	$RhC_4H_6^+$	56	H_2	$RhC_8H_{12}^+$
				$2H_2$	$RhC_8H_{10}^+$
	$2H_2$	$RhC_4H_4^+$	33	-	$RhC_8H_{12}^+$
				H_2	$RhC_8H_{10}^+$
	C_2H_4	$RhC_2H_4^+$	11	H_2	$RhC_6H_{10}^+$
				$2H_2$	$RhC_6H_8^+$
c-C_5H_{10}	$2H_2$	$RhC_5H_6^+$	100	$2H_2$	$RhC_{10}H_{12}^+$
c-C_6H_{12}	$2H_2$	$RhC_6H_8^+$	65	H_2	$RhC_{12}H_{18}^+$
				$2H_2$	$RhC_{12}H_{16}^+$
	$3H_2$	$RhC_6H_6^+$	35	H_2	$RhC_{12}H_{16}^+$

[a] Distribution of the primary products (RhA^+) is given in percent of the total primary products. [b] Major tertiary reaction also observed. See text for explanation.

reductive elimination of H_2. The resulting metal–alkyl intermediate C is very unstable with respect to β-H elimination[18] and loses H_2 again to form a second allyl ligand bound to the metal. When this reaction is carried out in the presence of excess D_2, $RhC_3H_6^+$ undergoes five H/D exchanges as shown in Figure 2 which is characteristic of the allyl hydride structure[19] and provides evidence for the mechanism shown in Scheme II. Similar behavior has been reported by Beauchamp et al.[20] who observed the following reaction using ICR spectrometry:

$$CpRhD^+ + C_3H_8 \rightarrow CpRh(C_3H_5)^+ + HD + H_2$$

The release of multiple hydrogens here is similar to the reaction of $RhC_3H_6^+$ and C_3H_8 and supports the concept of a metal hydride

---

(18) β-Hydride shifts are recognized as the major step in the decomposition of metal–alkyl bonds in solution: R. F. Heck, "Organotransition Metal Chemistry", Academic Press, New York, 1978, pp 45–54.

(19) See ref 10, pp 1231–1232.

(20) J. L. Beauchamp, A. E. Stevens, and R. R. Corderman, *Pure Appl. Chem.*, **51**, 967 (1979).

Scheme III

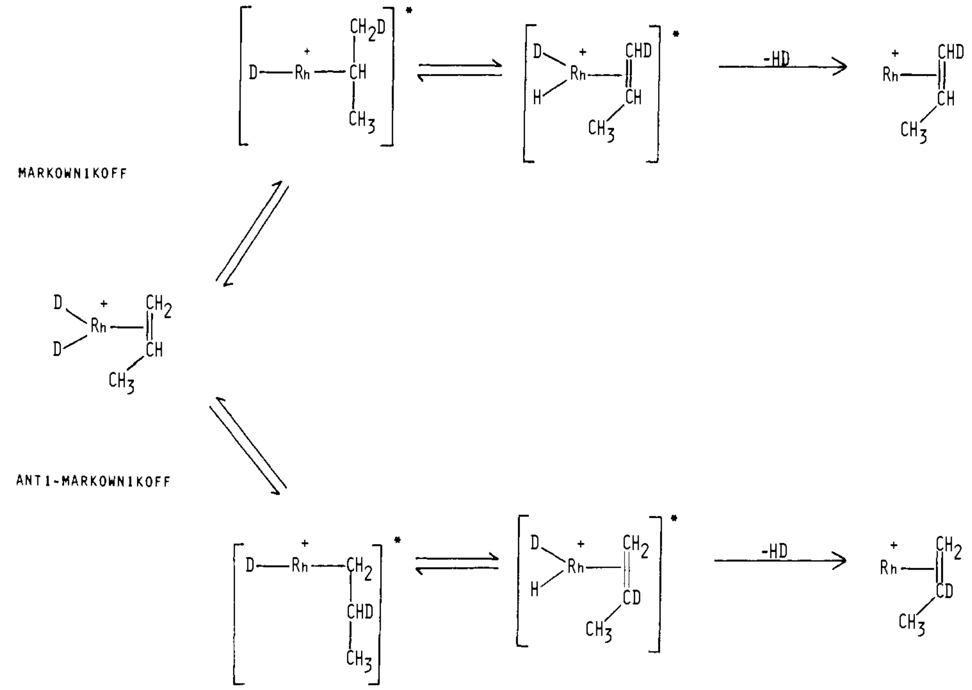

structure for $RhC_3H_6^+$. Also, the product in this reaction, $CpRh(C_3H_5)^+$, underwent only four H/D exchanges in the presence of D_2 which is compatible with our H/D exchange results. The unexchanged hydrogen in each case is the one attached to the center carbon as discussed below for the 2-methylpropane case.

Although other mechanisms are possible, it is difficult to explain the five H/D exchanges without invoking the allyl structure. For example, if the structure were simply a Rh^+–propene complex, direct addition of the metal across the double bond should result in both Markownikoff and anti-Markownikoff structures as illustrated in Scheme III. Thus, H/D exchange of all six hydrogens on $RhC_3H_6^+$ would be permitted but this is not observed. If Markownikoff addition was the only exchange mechanism, then one hydrogen would remain unexchanged. However, solution studies[21] indicate that the anti-Markownikoff addition is actually preferred because of steric reasons. Even though steric effects are less pronounced in these coordinatively unsaturated species, there is no logical reason to assume a pure Markownikoff addition. It is interesting to note that $CoC_3H_6^+$ formed from the reaction of Co^+ and C_3H_8 in the presence of D_2 does not undergo any H/D exchanges.[22]

2-Methylpropane yields two primary products and each reacts in the same manner with a second $i\text{-}C_4H_{10}$ to lose $2H_2$. By postulating a 2-methylallyl structure for $RhC_4H_8^+$, the double H_2 loss in the secondary reaction can be explained as in Scheme II. Again, by carrying out this reaction in excess D_2, eight H/D exchanges are seen for $RhC_4H_8^+$ as shown in Figure 3 which would be expected for a 2-methylallyl structure. In addition, since the substitution of a methyl group for a hydrogen in the C-2 position of the allyl structure results in the exchange of all eight hydrogens, this is proof that the lone unexchanged hydrogen in the allyl–metal hydride (structure B in Scheme II) is indeed the one attached to the middle carbon. The other primary ion, $RhC_4H_6^+$, shows no H/D exchanges and may be a 1,3-butadiene complex, as discussed below for *n*-butane.

***n*-Butane, *n*-Pentane, 2-Methylbutane, and 2,3-Dimethylbutane.** All of these alkanes containing a C_4 or C_5 chain lose $2H_2$ in both primary and secondary reactions, presumably to form 1,3-butadiene complexes (with the appropriate methyl substituents) bound to rhodium. Butadiene ligands have long been known to bind strongly to metal centers where they can undergo hydrogenation and isomerization.[23] The formation of 1,3-butadiene from *n*-butane can be seen as a logical extension of Scheme II where the intermediate analogous to B is not stable with respect to the transfer of a fourth hydrogen onto the metal and reductive elimination of the second H_2. These hydrogen transfers are very fast and no butene intermediates are seen on the time scale of the experiment. When excess D_2 is present, no H/D exchange occurs as would be expected for butadiene. The exothermic formation of $RhC_4H_6^+$ from *n*-butane implies $D(Rh^+–C_4H_6) > 56$ kcal/mol.[16] This result can be compared to $D(Co^+–C_4H_6) = 45–60$ kcal/mol previously determined.[5] The minor amounts of $RhC_3H_4^+$ and $RhC_3H_6^+$ formed in the reactions with *n*-pentane and 2-methylbutane could represent a competitive mechanism such as alkyl migration as discussed below for the reaction of 2,2-dimethylpropane or C–C insertion which is more common to the first-row group 8 metal ions. Of particular interest is the 4% of $RhC_5H_6^+$ formed in the reaction of Rh^+ with *n*-pentane. This may represent a dehydrocyclization reaction which is common for C_5 and C_6 hydrocarbons over supported metal catalysts as discussed below for *n*-hexane.

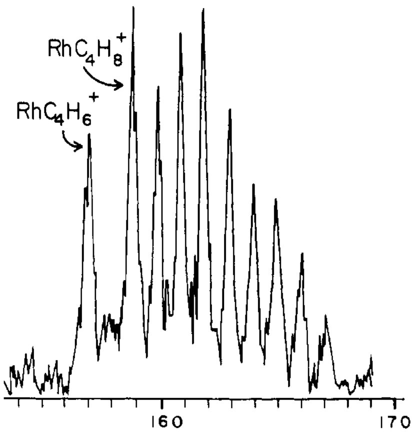

Figure 3. Expanded view of *m/z* 157 and *m/z* 159 resulting from the reaction of Rh^+ with 2-methylpropane. *m/z* 160 – *m/z* 167 appear only when excess D_2 is added to the system and represent a total of eight H/D exchanges for $RhC_4H_8^+$.

---

[21] See ref 10, 3rd ed., pp 789–790.

[22] G. D. Byrd and B. S. Freiser, unpublished results.

[23] Reference 10, 3rd ed., pp 731–733.

Scheme IV

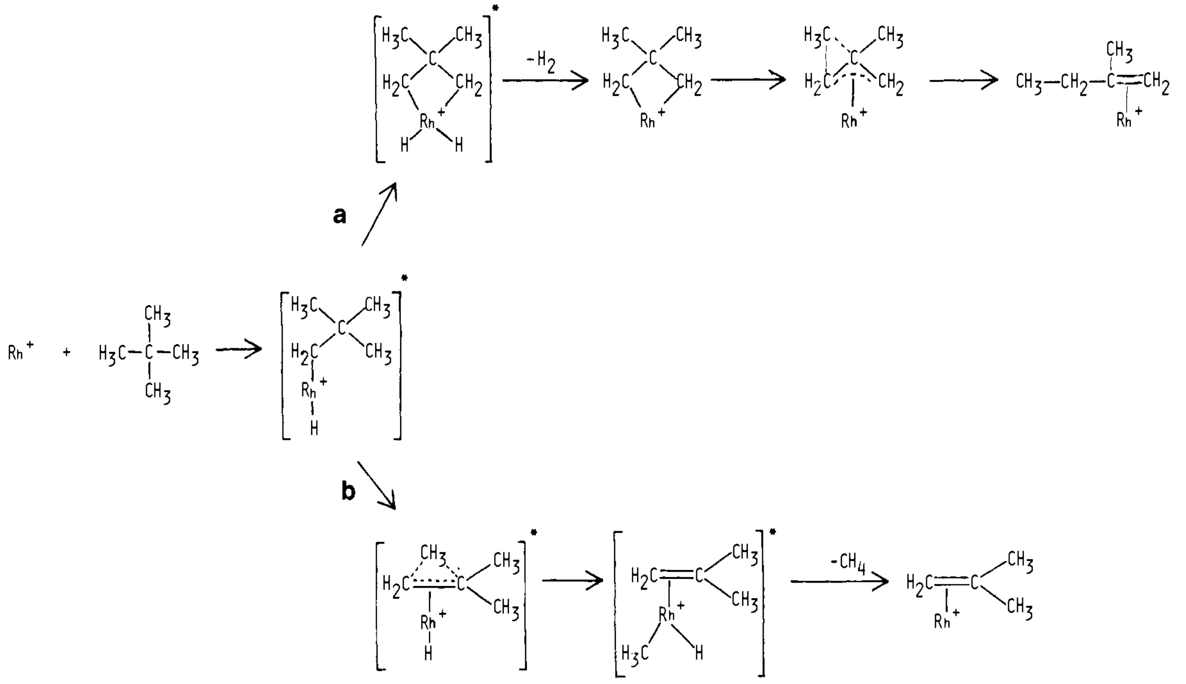

The secondary reactions of these diene complexes to attach another diene show that rhodium can insert into C–H bonds even with a four-electron-donating ligand attached. Rh$^+$, a d^8 metal ion, still requires six electrons to fill its valence shell when one butadiene is attached, based on the 18-electron rule. Thus, attachment of another electron-donating ligand is favorable on this basis, and any intermediate required to form a second diene is apparently not hampered sterically by the original butadiene.

***n*-Hexane, *n*-Heptane, and *n*-Octane.** These larger normal alkanes all show primary products with molecular formulas indicative of trienes bound to the metal as a result of 3H_2 loss. These primary complexes, in general, show little or no tendency to undergo secondary reactions with the original alkane. This behavior suggests that the rhodium center has attained a limit of electronic or steric saturation as a result of a bound triene. The *n*-heptane case illustrates this effect clearly where $RhC_4H_6^+$ reacts with *n*-heptane while $RhC_7H_{10}^+$ does not.

The primary reaction between *n*-hexane and Rh$^+$ shows 18% of the total reaction products as $RhC_6H_6^+$, representing a loss of 4H_2 from the initial collision complex. Assuming that $RhC_6H_6^+$ is a rhodium–benzene complex, then this represents a dehydrocyclization reaction. Dehydrocyclization of both C_5 and C_6 alkanes is an important process in the petrochemical industry, and the aromatization of *n*-hexane over supported metal catalysts is known.[24]

2,2-Dimethylpropane and 2,2-Dimethylbutane. 2,2-Dimethylpropane (neopentane) reacts with Rh$^+$ to produce a more complicated distribution of products than any other alkane in this study. This is due in part to its unusual structure where the center carbon in the C_3 chain has no hydrogens directly attached. This feature makes β-hydride shifts impossible for an initial C–H insertion into this structure. Since this very important mechanism is now blocked, other mechanisms must be considered. Isomerization of the carbon structure can be rationalized to explain $RhC_5H_{10}^+$, as shown in Scheme IV (path a), which has been postulated for the reaction of neopentane with platinum by Clarke and Rooney[25] and involves the formation of a metallocyclobutane intermediate. The resulting isopentene ligand can easily lose another H_2 to produce $RhC_5H_8^+$. Other types of rearrangements are also possible as shown in Scheme IV (path b) which is based on a mechanism postulated by Foger and Anderson[26] for the reaction of neopentane with platinum and argues for a 1,2-alkyl shift to account for the C_4 ligands from neopentane. By increasing the C_3 chain to C_4 in going to 2,2-dimethylbutane, the number of major primary (>10% of the total intensity) reactions are lowered. This simplification is due mainly to the reinstatement of a plausible β-H shift without rearrangement of the carbon skeleton. However, since there is still a carbon with no hydrogens directly bound, some of the same competitive mechanisms as in the neopentane case may be involved. It is interesting to note that the two most intense primary ions in each case have molecular formulas that correspond to dienes bound to the metal.

Cyclopropane and Cyclobutane. Unlike the larger cyclic alkanes, these smaller cyclic alkanes exhibit noticeable amounts of ring cleavage products in their primary reactions with Rh$^+$. Although the major primary ions do not involve the loss of any ring carbons from the collision complex, some of the observed carbon-containing losses are unique to the overall trends in Rh$^+$/alkane reactions.

The major reaction for cyclopropane produces $RhC_3H_4^+$ which reacts a second time to produce $RhC_6H_6^+$. This product reacts yet a third time with cyclopropane to yield $RhC_9H_{10}^+$, by far the dominant ion in the spectrum after a few seconds. $RhC_3H_4^+$ appears in minor amounts in many of the reactions listed in Table I. It is very similar in behavior to $RhC_3H_6^+$ in that it loses 2H_2 in its secondary reaction and all four hydrogens undergo H/D exchange. Thus, a possible structure would be the metal hydride, $HRhC_3H_3^+$, but it is not known whether the C_3 ring maintains its integrity or expands to form a metallocyclobutane with the rhodium. The $RhC_3H_6^+$ formed by direct attachment may be stabilized by a rearrangement to propene via a π-allyl hydride intermediate or may involve a metallocyclobutane as suggested by Armentrout and Beauchamp for the analogous reaction with Co$^+$.[27] This rearrangement is favorable since the heat of formation of propene is 7.86 kcal/mol less than that of cyclopropane.[28] The secondary reaction of $RhC_3H_6^+$ formed here produces $RhC_6H_{10}^+$ which is also similar to the $RhC_3H_6^+$ formed from propane and suggests that both ions have similar structures. Deuterium exchange on $RhC_3H_6^+$ from cyclopropane was inconclusive because of its weak intensity relative to $RhC_3H_4^+$. The

---

(24) F. G. Ciapetta and D. N. Wallace, *Catal. Rev.*, **5**, 67 (1971).

(25) J. K. A. Clarke and J. J. Rooney, *Adv. Catal.*, **23**, 1 (1973).

(26) K. Foger and J. R. Anderson, *J. Catal.*, **54**, 318 (1978).

(27) P. B. Armentrout and J. L. Beauchamp, *J. Chem. Phys.*, **74**, 2819 (1981).

(28) Based on data for the heats of formation of these neutrals taken from ref 16.

(29) A. Efraty, *Chem. Rev.*, **77**, 691 (1977).

production of $RhCH_2^+$ is interesting since formation of the metal carbene $CoCH_2^+$ was reported as the major reaction between Co^+ and cyclopropane in an ion beam instrument,[27] although the Co^+ reaction was slightly endothermic.

It is difficult to explain $RhC_2H_4^+$ produced by the reaction of cyclobutane with Rh^+ without invoking a C–C insertion by the metal such as that proposed for the reaction of Co^+ with cyclobutane.[7b] Opening of the ring may also occur in the major reaction to form $RhC_4H_6^+$. It has long been known that transition metals can stabilize cyclobutadiene[24] which may be the case in the formation of $RhC_4H_4^+$. The observation of only H_2 loss in the secondary reaction suggests that the C_4 unit in this complex remains intact either as the original C_4 ring or as a metallocyclic species.

Cyclopentane and Cyclohexane. These larger cyclic alkanes gave no ring cleavage products (i.e., neutral alkene loss) on primary reaction with Rh^+, and both showed the loss of 2- or $3H_2$. The absence of any ions with masses between those of the primary and secondary products for these systems gives further evidence that the ring structures remain intact as the original C_5 and C_6 rings or as metallocycles. If $RhC_5H_6^+$ formed from cyclopentane was actually $HRhCp^+$, then some deuterium exchange might be expected, but none was observed when this reaction was carried out in excess D_2.

Conclusion

Rh^+ behaves much like Ti^+ in its primary[30] and secondary[22] reactions with alkanes where dehydrogenation resulting from C–H insertion is by far the dominant reaction. This contrasts sharply with the first-row group 8 transition metal ions which show extensive C–C cleavage products when reacted with these same alkanes.[5,30,31] In particular, the differences between Co^+ and Rh^+ show that significantly different trends in reactivity can occur for two members of the same group. As an example, Co^+ reacts with cyclopentane and cyclohexane to produce the ring cleavage product $CoC_3H_6^+$ as a major ion in both instances which is in sharp contrast to the dehydrogenation reactions of Rh^+. The underlying reason for these differences is probably the inability of Rh^+ to readily insert into C–C bonds. Ethylene and butadiene bonding energies to both Co^+ and Rh^+ appear comparable, however.

π-Allylic species are often postulated for many hydrocarbon reactions over metal catalysts and figure prominently in our gas-phase mechanisms. The existence of other π–fluxional–π structures[32] such as $HRhC_3H_3^+$ and $HRhCp^+$ are considered probable. We are currently investigating the structures of these complexes in more detail.

The Rh^+–alkane systems reach a point where secondary reactions are no longer observed for large, highly unsaturated primary products. This condition occurs for ions with molecular formulas corresponding to triene-bound rhodium complexes. Both steric and electronic effects may contribute to this phenomenon.

It should be noted that certain Rh(I) complexes such as $RhCl(PPh_3)_3$ are not observed to dehydrogenate alkanes.[33] The reason for this difference between gas-phase and solution results is twofold. First, the complex formed by an ion–molecule collision in the gas phase is activated with excess internal energy that can allow for an oxidative addition by the metal to a carbon–hydrogen bond. This energy is rapidly dissipated in solution by the solvent molecules. Secondly, the bare atomic metal ion in the gas phase has many sites available to the alkane while complexed metals are shielded by their ligands.

Acknowledgment is made to the Department of Energy (DEAC02-80ER10689) for supporting this research and the National Science Foundation for providing funds to purchase the FTMS. In addition, one of us (G.D.B.) thanks Chevron for providing fellowship support. We also thank Professors Cliff Kubiak and Ian Rothwell, Chemistry Department, Purdue University, for their helpful discussions.

Registry No. Rh^+, 20561-59-5; CH_4, 74-82-8; C_2H_6, 74-84-0; C_3H_8, 74-98-6; n-C_4H_{10}, 106-97-8; i-C_4H_{10}, 75-28-5; n-C_5H_{12}, 109-66-0; i-C_5H_{12}, 78-78-4; *neo*-C_5H_{12}, 463-82-1; n-C_6H_{14}, 110-54-3; $(CH_3)_2CHCH(CH_3)_2$, 79-29-8; $(CH_3)_3CCH_2CH_3$, 75-83-2; n-C_7H_{16}, 142-82-5; n-C_8H_{18}, 111-65-9; cyclo-C_3H_6, 75-19-4; cyclo-C_4H_8, 287-23-0; cyclo-C_5H_{10}, 287-92-3; cyclo-C_6H_{12}, 110-82-7.

---

(30) G. D. Byrd, R. C. Burnier, and B. S. Freiser, *J. Am. Chem. Soc.*, **104**, 3565 (1982).

(31) L. F. Halle, P. B. Armentrout, and J. L. Beauchamp, *J. Organomet. Chem.*, submitted.

(32) For a general discussion of these structures, see ref 10, 3rd ed., pp 36–46, 761–767.

(33) J. A. Osborn, F. H. Jardine, J. F. Young, and G. Wilkinson, *J. Chem. Soc. A*, 1711 (1966).